Rev. Roum. Sci. Techn.– Électrotechn. et Énerg.
Vol. **65**, *1-2*, pp. 67–70, Bucarest, 2020

Dedicated to the memory of Academician Gleb Drăgan

PERFORMANCE EVALUATION OF PHOTOVOLTAIC PANELS CONTAINING CELLS WITH DIFFERENT BUS BARS CONFIGURATIONS IN PARTIAL SHADING CONDITIONS

GEORGE CALIN SERITAN[1], BOGDAN-ADRIAN ENACHE[1], FELIX-CONSTANTIN ADOCHIEI[1], FLORIN-CIPRIAN ARGATU[1], CHRISTOS CHRISTODOULOU[2], VASILIKI VITA[2], ANA RUXANDRA TOMA[1], COSTIN HEDWIG GANDESCU[1], FRANCISC - IOAN HATHAZI[3]

Key words: Photovoltaic panel, Bus bar, One diode model, Partial shading.

One factor that drastically limited the penetration level of photovoltaic (PV) panels into the market was their low performance in partial shading conditions (PSC). When the cells from a panel receive different amounts of irradiations, the maximum power generation capability of the panel is impacted, and the entire performance is reduced. Several techniques were employed to overcome this phenomenon i.e. bypass diodes, different cells interconnections, cooling solutions, etc. In this study, we analyze the effect of partial shading over PV panels containing cells with different bus bars (BB) configurations. This is important because it can help designers choose the most appropriate type of cell for areas that are more prone to PSC and it can also be useful for other studies to improve the performances of new types of cells.

1. INTRODUCTION

From its early beginning, the PV panel carried a heavy burden, its theoretical conversion efficiency limit set by Shockley and Queisser (S-Q limit) to 30 %. While this limit was latter updated to 33.7 % due to more accurate calculations of the band gap energy, it is still considered a low performance compared to other p-n junction devices [1]. With all this, the PV panel made great progress in both directions: scientific research and commercial applications, the latter being the driving force of the industry.

Today, PV deployment is over 500 GW spread all over the Globe and will continue to grow back-up by programs like: European Fund for Strategic Investments (EFSI), Horizon 2020 (European Union), Tesla Solar Roof (United States), Smart Export Guarantee (United Kingdom) *etc* [2]. These programs make the higher level of penetration for PV possible, although the price for polysilicon rebounded 6 % from last year reaching 9.20 $/kg, and the average selling price for PV panels in July 2019 was 0.26 $/W identical to the price from the same period of 2018 [3, 4].

The scientific research for PV panels is mostly concentrated around materials for the cells itself, the bonding adhesives, the glass *etc*. Typically, a PV cell is a thin wafer consisting of a thin layer of phosphorous-doped (N-type) silicon placed on top of a thicker layer of boron-doped (P-type) silicon. The most common materials used for manufacturing PV cells are monocrystalline silicon, polycrystalline silicon and amorphous silicon. In laboratory conditions, crystalline Si PV cells reached a maximum efficiency rate of 26.7 % [5]. New materials like organic cells, group III-V materials and perovskite cells are undergoing rapid development to push the efficiency rate closer to the S-Q limit [5].

In a parallel direction, the structure of a PV cell also evolved. The first generation of commercially available cells used a rectangular shape and one or two BB to collect the generated current (Fig. 1).

Current cells are designed to maximize the surface area exposed to the Sun while minimizing the resistance of the current path. Commonly, they have a square shape of around 15 x 15 cm, and 2 to 5 BB (Fig. 2 a) – d)). The 4 and 5 BB cells are available in two types with full BB or with slotted ones (Fig. 2 e) – f)). We will present all the commercially available PV cells with 2 to 5 BB in both forms in this paper.

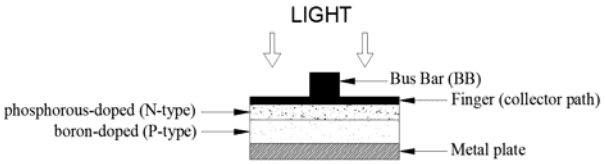

Fig. 1 – Structure of a PV cell.

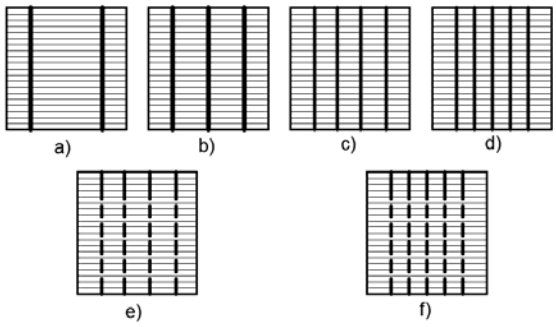

Fig. 2 – Cells with different BB configurations.

During this study, we discover that there is one Indian manufacturer who delivers PV cells with 6 and 12 BB, but there is insufficient data to include these cells in our article.

In PSC, PV cells from a panel receive different amounts of solar irradiation. Shadows can be cast by clouds, poles, trees, buildings, birds or accumulation of dust and residues on the PV cells. Except for fixed structures, most of the times the shadows cannot be predicted, but in all the cases their impact over the performance of the PV panel is significant. One study [6] proves that a 2 % area of a module shaded can lead to almost 70 % performance loss, while others [7, 8] showed that 5–10 % panel shade reduces

[1] University "Politehnica" of Bucharest, Faculty of Electrical Engineering, Spaiul independentei 313, Bucharest, Romania, E-mail:bogdan.enache2207@upb.ro
[2] Department of Electrical and Electronic Engineering Educators, A.S.PE.T.E.—School of Pedagogical and Technological Education, Athens, Greece,E-mail: christ_fth@yahoo.gr
[3] Electrical Engineering Department, Faculty of Electrical Engineering and Information Technology, Oradea, Bihor, Romania

the output power up to 80 %. The common denominator of these studies is that the power losses caused by shading, depend both on the covered area of a cell and the percentage of the shaded cells from the panel together with the cell type.

The shadows affect not only the current flow in the cell, but they also limit the current flow in the whole panel because most of the times cells are connected in series. On the other hand, if the shaded cells are forced to conduct more current, they will get reverse biased which will increase the thermal stress and lead to the formation of hot-spots [9]. Usually, this is avoided by connecting bypass diodes antiparallel with every cell, which provide an alternate path for the current [10, 11]. In practice, PV panels are equipped with either only one bypass diode for every 12 to 18 cells or none at all [12].

Another way that the effect of PSC can be reduced, is by using different connections schemes like: total-cross-tied (TCT), Bridged-Linked (BL), and Honey-Comb (HC) [13–15], beside the classic ones: series, parallel and SP. Also, several studies [16–20], investigated reconfiguration schemes by which shaded cells are rearranged inside the panel and so improving the efficiency of the system.

This paper extends the research done by the authors in [21], where only one cell was investigated. Now, we analyze the effect of PSC over a string of 5 cells connected in series with different BB configurations. The goal is to evaluate the performance of the proposed PV panels in PSC. The main contributions of the paper are:

- developing the model for 2 to 5 BB cells based only on the manufacturer data (Section 2);
- creating a realistic scenario for a casting shadow that affects 5 cells connected in series (Section 3);
- determining the efficiency of the proposed panels by direct comparison of the maximum power point (MPP) from standard test conditions (STC) with the MPP from PSC (Section 4).

2. PV CELL MODEL

A lot of models have been developed in order to simulate the performance of a solar cell because a practical analysis is expensive and difficult due to the changing environmental conditions. Most of them use equivalent circuit models based on a diode placed in parallel with a current source (ideal model), to define the entire *I-V* characteristic of the cell for a given set of operating conditions. Among them, the single-diode model and the two-diode model are a preferred choice because they offer excellent accuracy with minimal computational effort [22, 23]. In this study, we will use the one diode model due to the limited data provided by the manufacturer (only the *I-V* curve for STC), and because it offers a good compromise between accuracy and complexity.

2.1. ONE DIODE MODEL

The one diode model extends the ideal model of a PV cell by adding a series and parallel resistor.

The equation that describes the output current I, of the cell, is given by eq. (1):

$$I = I_{ph} - I_0\left[\exp\left(\frac{q\cdot(V + I\cdot R_s)}{A\cdot k_B\cdot T}\right) - 1\right] - \frac{V + I\cdot R_s}{R_p}, \quad (1)$$

where I_{ph} is the photocurrent, I_0 is the diode saturation current, A the diode ideality factor, q the elementary charge, k_B the Boltzmann constant, T the temperature in K, V the output voltage, R_s and R_p the shunt and parallel resistors.

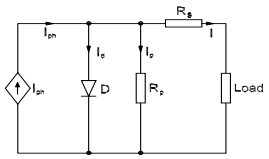

Fig. 3 – One diode model

All the parameters from eq. (1) are temperature dependent, but in this study, we choose to neglect this effect in order to reduce the complexity of the model. The diode ideality factor was set to 1.3 which is a good approximation for a Si-poly crystalline cell [24].

2.2. PARAMETER EXTRACTION

Considering eq. (1), the parameters needed for the implementation of the model are: the photocurrent, the diode saturation current, the series and parallel resistors and the diode ideality factor – 5 parameters model. There are several methods, presented in the literature, to determine these parameters: iterations methods [24], graphic methods [22], and adaptive techniques [25] *etc*. In this paper, due to the limited data provided by the manufacturer, we use a graphic method that requires as input only the *I-V* characteristic of the cell at STC. This method considers the coordinates of 4 points on the *I-V* characteristic: (VOC, 0), (V_1, I_1), (V_2, I_2) and (0, I_{sh}) (Fig. 4), and based on them determines the slopes of the current and voltage sources parts, that are used to calculate the values for R_s and R_p [25]. The rest of the parameters are calculated using well-known equations available in the literature.

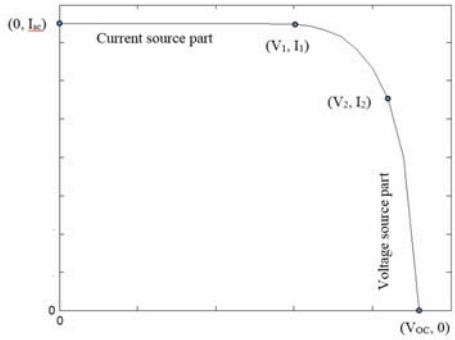

Fig. 4 – The graphic method used to extract model parameters.

3. THE SHADOW SCENARIOS

The shadow scenarios are based on a real case in which a stairs shaped building with several floors is casting a shadow to a string of 5 series connected PV cells placed facing South. The moving shadow is progressive and affects the cells from bottom to top. Considering the trajectory of the Sun from left to right, at 11 o'clock the shadow affects only the cell number 2 covering 10 % of its effective area (Fig. 5 a)). At 12 o'clock the shadow affects cells numbers 2 and 3 covering 15 % of each cell (Fig. 5 b)). At 13 o'clock the shadow is at its peak covering cell

no. 2 – 20 %, cell number 3 (25 %), cell number 4 (15 %) (Fig. 5 c)).

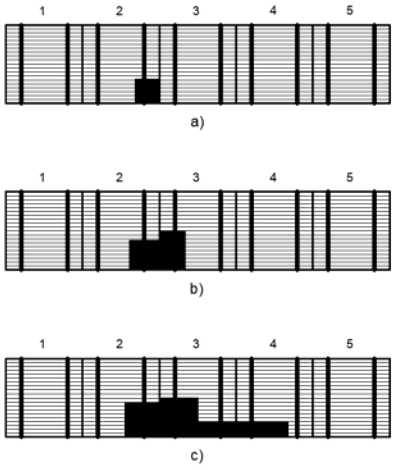

Fig. 5 – Shadow patterns.

The correlation between the shadow patterns and the level of irradiance that reaches each cell is done by using the covered area coefficient [18, 7] and the limit values of irradiance from the manufacturer data-sheet at STC. When the PV cell is not covered, the irradiance level is maximum *i.e.* 1000 W/m^2, while when it is covered entirely its irradiance level drops to 200 W/m^2 [26– 28]. Between these two extreme points, the irradiance values for the scenarios presented earlier are shown in Table 1.

Table 1

Covered area coefficient correlated with irradiance level

Covered area [%]	Irradiance level [W/m^2]
10	920
15	880
20	840
25	800

4. RESULTS AND DISCUSSION

The cells stimulated in this study are based on the data sheets provided by Topsky Energy (HK) Limited, a Chinese Hong Kong-based manufacturer. This manufacturer was chosen because it produces the entire set of cells from 2 BB to 5 BB that have relative close MPPs (Table 2).

Table 2

PV cells manufacturer data

Characteristic	2 BB	3 BB	3 BB with slots
Dimensions [mm]	156.75×156.75	156.75×156.75	156.75×156.75
No. of bus bars	2	3	3
Width [mm]	1.8	1.5	1.5
Maximum power [W]	4.42	4.47	4.429
***V* MPP [V]**	0.523	0.535	0.535
***I* MPP [A]**	7.925	8.26	8.28
VOC [V]	0.647	0.636	0.64
ISC [A]	8.642	8.77	8.66
4 BB	**4 BB with slots**	**5 BB**	**5 BB with slots**
156.75×156.75	156.75×15675	156.75×156.75	156.75×156.75
4	4	5	5
0.7	1	0.7	0.8
4.429	4.67	4.42	4.53
0.527	0.56	0.535	0.542
8.456	8.34	8.22	8.35
0.633	0.663	0.626	0.639
8.991	9.07	8.85	8.85

Based on the data from Table 2 and applying eq. (1) and the methodology presented in Section 2, we developed the models for the 2 BB, 3 BB, 4 BB and 5 BB PV cells at STC, *i.e.* T = 25 °C, and I = 1000 W/m^2 (Fig. 6).

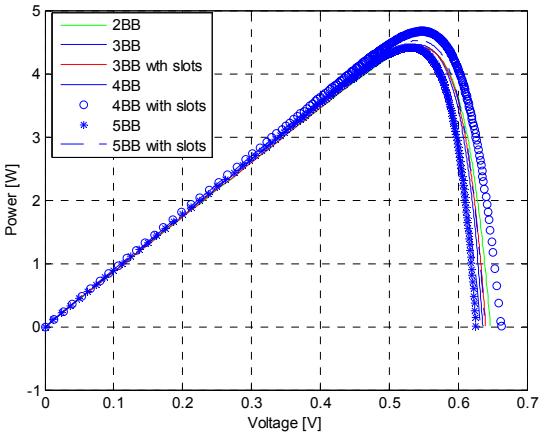

Fig. 6 – PV cells characteristics at STC.

The differences at MPP between the developed models and the manufacturer data are below 2 %. Due to the fact that cells with lower Rs are more prone to produce hot-spots in a string formation, we present the values obtained through simulation for a single cell in Table 3.

Table 3

PV cells Rs

Parameter	2 BB	3 BB	3 BB slots
Rs [mΩ]	1.1	1.0	2.4
4 BB	**4 BB slots**	**5 BB**	**5 BB slots**
1.78	2.5	1.0	1.3

In the next phase of the study, we connected 5 PV cells of the same type, determined their effective exposed area (Table 4), and submitted them to the proposed scenarios.

Table 4

Effective exposed areas of the PV cells

Characteristics	2 BB	3 BB	3 BB slots
Cell area [mm^2]	24570.56	24570.56	24570.56
BB area [mm^2]	564.3	705.375	423.22
BB area [%]	2.296	2.870	1.722
Effective area [%]	97.703	97.129	98.278
4 BB	**4 BB slots**	**5 BB**	**5 BB slots**
24570.56	24570.56	24570.56	24570.56
438.9	376.2	548.625	376.2
1.786	1.531	2.232	1.531
98.214	98.469	97.767	98.469

Based on the effective exposed areas and the correlation between the irradiance and exposed areas, we determined the MPP for each PV panel at STC, which will act as a reference for the efficiency evaluation. For the proposed scenarios we calculated the partial shading power losses (PSPL) and the fill factor (FF) (Table 5).

The PSPL is obtained by subtracting the MPP at PSC from the value of MPP at STC – eq. (2). The FF depends on the open-circuit voltage, short circuit current and MPP at PSC –eq. (3).

$$\mathrm{PSPL} = \mathrm{MPP}_{\mathrm{STC}} - \mathrm{MPP}_{\mathrm{PSC}}, \tag{2}$$

$$\mathrm{FF} = \frac{\mathrm{MPP}_{\mathrm{PSC}}}{Vo_C \cdot I_{\mathrm{SC}}} \cdot 100. \tag{3}$$

Table 5

PV panel performances under PSC

Characteristics		2 BB	3 BB	3 BB s
No. shade	MPP_{STC} [W]	21.57	21.63	21.72
Scenario 1	PSPL [W]	0.66	0.68	0.68
	FF [%]	74.79	75.12	75.92
Scenario 2	PSPL [W]	1.73	1.74	1.73
	FF [%]	70.96	71.31	72.13
Scenario 3	PSPL [W]	3.18	3.15	3.23
	FF [%]	65.77	66.26	66.72

Table 5 – continuation

Characteristics		4 BB	4 BB s	5 BB	5 BB s
No. shade	MPP_{STC} [W]	21.73	22.97	21.58	22.24
Scenario 1	PSPL [W]	0.65	0.68	0.67	0.67
	FF [%]	74.07	74.13	75.48	76.28
Scenario 2	PSPL [W]	1.68	1.79	1.71	1.77
	FF [%]	70.45	70.44	71.73	72.39
Scenario 3	PSPL [W]	3.14	3.31	3.21	3.31
	FF [%]	65.32	65.38	66.31	66.94

The cell that exhibits the lowest power losses for all the three scenarios is the 4BB cell, which registered a power loss between 0.65 – 3.14 W for the regular version and 0.68 – 3.31 W for the slotted one. At the opposite pole is the 2 BB cell with registered power loses between 0.66 – 3.18 W.

Regarding the FF, the best cell is the 5BB which has the biggest values between 75.48 – 66.31 % for the regular version and 76.28 – 66.94 % for the slotted version. The lowest FF is achieved by the 4 BB cell with values between 65.32 – 74.07 % (regular version) and 65.38 – 74.13 % (slotted version). This can be explained considering the increased values of the internal resistance of the 4 BB cell which lowers its efficiency overall.

4. **CONCLUSIONS**

This paper analyzes 7 types of poly-Si PV cells connected in series and submitted to a live PSC scenario. The cells have different BB configuration which leads to different internal resistances and effective exposed areas.

Regarding the number of BB, our study concluded that the 5 BB cell is the most efficient in PSC, followed by the 3 BB and the 4 BB ones.

The new technology of slotted BB while emphasizing the effective exposed area over the internal resistance, showed that if these values are not carefully chosen, they produce worse results then the full BB. This proves that the performance of a cell is given by a perfect balance between effective exposed area and internal resistance.

Received on November 11, 2019

REFERENCES

1. T. Ma, Z. Li, J. Zhao, *Photovoltaic panel integrated with phase change materials (PV-PCM): technology overview and materials selection*, Renew. Sustain. Energy Rev., **116**, p. 109406, 2019.
2. M. Q. Duong, N. Thien, N. A. M. Tran, G. N. Sava, V. Tanasiev, *Design, performance and economic efficiency analysis of the photovoltaic rooftop system*, Rev. Roum. Scie. – Techn. Électrotechn. et Énerg., **64**, *3*, pp. 229–234 (2019).
3. M. R. Feldman David, *Q1/Q2 2019 Solar Industry Update*, NREL, 2019.
4. M. R. Feldman David, *Q1/Q2 2018 Solar Industry Update*, NREL, 2018.
5. A. Polman, M. Knight, E. C. Garnett, B. Ehrler, W. C. Sinke, *Photovoltaic materials: Present efficiencies and future challenges*, Science, **352**, *6283*, p. aad4424 (2016).
6. V. Quaschning, R. Hanitsch, *Numerical simulation of current-voltage characteristics of photovoltaic systems with shaded solar cells*, Sol. Energy, **56**, *6*, pp. 513–520 (1996).
7. J. Viitanen *et al*., *Energy efficient lighting systems in buildings with integrated photovoltaics*, PhD Thesis, Aalto University, 2015.
8. G. Seritan, I. Tristiu, G. Fierascu, R. Vatu, *Assessment for Efficient Operation of Smart Grids Using Advanced Technologies*, International Conference and Exposition on Electrical And Power Engineering (EPE), 2018, pp. 901–905.
9. A. M. Nader, D. Abderrahmane, *Direct power control for a photovoltaic conversion chain connected to a grid*, Rev. Roum. Scie. – Techn. Électrotechn. et Énerg., **61**, *4*, pp. 378–382 (2016).
10. S. Silvestre, A. Boronat, A. Chouder, *Study of bypass diodes configuration on PV modules*, Appl. Energy, **86**, *9*, pp. 1632–1640 (2009).
11. O. Ceaki, G. Seritan, R. Vatu, M. Mancasi, A*nalysis of power quality improvement in smart grids*, 10th International Symposium on Advanced Topics in Electrical Engineering (ATEE), 2017, pp. 797–801.
12. S. Malathy, R. Ramaprabha, *A static PV array architecture to enhance power generation under partial shaded conditions*,Proc. Int. Conf. on Power Electron. Drive Syst., June 9-12, pp. 341–346, 2015.
13. O. Bingöl, B. Özkaya, A*nalysis and comparison of different PV array configurations under partial shading conditions*, Sol. Energy, **160**, pp. 336–343 (2018).
14. F. Belhachat, C. Larbes, A *review of global maximum power point tracking techniques of photovoltaic system under partial shading conditions*, Renew. Sustain. Energy Rev., **92**, pp. 513–553 (2018).
15. S. R. Pendem, S. Mikkili, *Performance evaluation of series, series-parallel and honey-comb PV array configurations under partial shading conditions*, 7th Int. Conf. Power Syst. ICPS 2017, pp. 749–754, 2018.
16. P. R. Satpathy, S. Jena, R. Sharma, *Power enhancement from partially shaded modules of solar PV arrays through various interconnections among modules*, Energy, **144**, pp. 839–850 (2018).
17. P. Srinivasa Rao, G. Saravana Ilango, C. Nagamani, M*aximum power from PV arrays using a fixed configuration under different shading conditions*, IEEE J. Photovoltaics, **4**, *2*, pp. 679–686 (2014).
18. A. Kumar, R. K. Pachauri, Y. K. Chauhan, *Experimental analysis of SP/TCT PV array configurations under partial shading conditions*, 1st IEEE Int. Conf. Power Electron. Intell. Control Energy Syst. ICPEICES, Delhi, India, 4-6 July 2016.
19. A. Tabanjat, M. Becherif, D. Hissel, *Reconfiguration solution for shaded PV panels using switching control*, Renew. Energy, **82**, pp. 4–13 (2015).
20. M. Baka, P. Manganiello, D. Soudris, F. Catthoor, *A cost-benefit analysis for reconfigurable PV modules under shading*, Sol. Energy, **178**, pp. 69–78 (2019).
21. G. Seritan, *et. al.*, P*erformance Evaluation of a Partially Shaded PV cell with Different Bus Bars Configurations*, UPEC Proceedings, Bucharest, 2019.
22. N. Barth, R. Jovanovic, S. Ahzi, M. A. Khaleel, *PV panel single and double diode models: Optimization of the parameters and temperature dependence*, Sol. Energy Mater. Sol. Cells, **148**, pp. 87–98 (2016).
23. S. Mirić, M. Nedeljković, *The solar photovoltaic panel simulator*, Rev. Roum. Scie. – Techn. Électrotechn. et Énerg., **60**, *3*, pp. 273–281 (2015).
24. B. Habbati, Y. Ramdani, Fatima Moulay, *A detailed modeling of photovoltaic module using MATLAB*, NRIAG J. Astron. Geophys., **3**, *1*, pp. 53–61 (2014).
25. B.-A. Enache, F.-M. Birleanu, M. Radut, *Modeling a PV panel using the manufacturer data and a hybrid adaptive method*, 8th International Conference on Electronics, Computers and Artificial Intelligence (ECAI), Ploiesti, Romania, 2016, pp. 1–6.
26. Marilena Stanculescu, S. Marinescu, G. Cheregi, *Matlab in electrical engineering*, J. of Electrical & Electronics Engineering, **2**, *2* (2009).
27. C.A. Christodoulou, L. Ekonomou, I.F. Gonos, N.P. Papanikolaou, *Lightning protection of PV systems*, Energy Systems, **7**, *3* (2015).
28. O. Ceaki, R. Vatu, M. Mancasi, R. Porumb, G. Seritan, *Analysis of electromagnetic disturbances for grid-connected PV plants*, Modern Electric Power Systems (MEPS), 2015.